

# Interaction of Tetraspan(in) TM4SF5 With CD44 Promotes Self-Renewal and Circulating Capacities of Hepatocarcinoma Cells

Doohyung Lee,<sup>1</sup> Juri Na,<sup>2\*</sup> Jihye Ryu,<sup>1\*</sup> Hye-Jin Kim,<sup>1\*</sup> Seo Hee Nam,<sup>3</sup> Minkyung Kang,<sup>1,4</sup> Jae Woo Jung,<sup>3</sup> Mi-Sook Lee,<sup>1</sup> Haeng Eun Song,<sup>1</sup> Jungeun Choi,<sup>3</sup> Gyu-Ho Lee,<sup>1</sup> Tai Young Kim,<sup>1</sup> June-Key Chung,<sup>2,5</sup> Ki Hun Park,<sup>6</sup> Sung-Hak Kim,<sup>7</sup> Hyunggee Kim,<sup>7</sup> Howon Seo,<sup>8</sup> Pilhan Kim,<sup>8</sup> Hyewon Youn,<sup>2,5</sup> and Jung Weon Lee<sup>1,3</sup>

Tumor metastasis involves circulating and tumor-initiating capacities of metastatic cancer cells. Epithelial-mesenchymal transition (EMT) is related to self-renewal capacity and circulating tumor cell (CTC) characteristics for tumor metastasis. Although tumor metastasis is a life-threatening, complicated process that occurs through circulation of tumor cells, mechanistic aspects of self-renewal and circulating capacities have been largely unknown. Hepatic transmembrane 4 L six family member 5 (TM4SF5) promotes EMT for malignant growth and migration, so it was rationalized that TM4SF5, as a hepatocellular carcinoma (HCC) biomarker, might be important for metastatic potential. Here, self-renewal capacity by TM4SF5 was mechanistically explored using hepatocarcinoma cells with or without TM4SF5 expression, and we explored whether they became CTCs using mouse liver-orthotopic model systems. We found that TM4SF5-dependent sphere growth correlated with CD24<sup>-</sup>, aldehyde dehydrogenase (ALDH) activity, as well as a physical association between CD44 and TM4SF5. Interaction between TM4SF5 and CD44 was through their extracellular domains with *N*-glycosylation modifications. TM4SF5/CD44 interaction activated proto-oncogene tyrosine-protein kinase Src (c-Src)/signal transducer and activator of transcription 3 (STAT3)/Twist-related protein 1 (Twist1)/B-cell-specific Moloney murine leukemia virus integration site 1 (Bmi1) signaling for spheroid formation, whereas disturbing the interaction, expression, or activity of any component in this signaling pathway inhibited spheroid formation. In serial xenografts using 200~5,000 cells per injection, TM4SF5-positive tumors exhibited subpopulations with locally increased CD44 expressions, supporting for tumor cell differentiation. TM4SF5-positive, but not TM4SF5- or CD44-knocked-down, cells were identified circulating in blood 4-6 weeks after orthotopic liver injection using *in vivo* laser scanning endomicroscopy. Anti-TM4SF5 reagent blocked their metastasis to distal intestinal organs. **Conclusion:** TM4SF5 promotes self-renewal and CTC properties supported by TM4SF5<sup>+</sup>/CD44<sup>+(TM4SF5-bound)</sup>/ALDH<sup>+</sup>/CD24<sup>-</sup> markers during HCC metastasis. (HEPATOLOGY 2015;61:1978-1997)

Hepatocellular carcinoma (HCC) is the third-most common cause of mortality resulting from cancer.<sup>1</sup> Although hepatic resection and liver transplantation represent first-line treatments for

HCC,<sup>2</sup> the second-line treatment for HCC patients in advanced stages has shown limited efficacy.<sup>3</sup> Moreover, metastatic recurrence renders this carcinoma resistant to any significant chemopreventive effects.

Abbreviations: Ab, antibody; ALDH, aldehyde dehydrogenase; Bmi1, B-cell-specific Moloney murine leukemia virus integration site 1; CSCs, cancer stem cells; c-Src, proto-oncogene tyrosine-protein kinase Src; CTC, circulating tumor cell; DAPI, 4',6-diamidino-2-phenylindole; DMSO, dimethyl sulfoxide; EGF, epidermal growth factor; EMT, epithelial-mesenchymal transition; FACS, fluorescence-activated cell sorting; FAK, focal adhesion kinase; FBS, fetal bovine serum; FCM, flow cytometry; HCC, hepatocellular carcinoma; IHC, immunohistochemistry; mRNA, messenger RNA; PBS, phosphate-buffered saline; RT-PCR, reverse-transcription polymerase chain reaction; shRNA, short hairpin RNA; Smad, small mothers against decapentaplegic; STAT3, signal transducer and activator of transcription 3; TEMs, tetraspan(in)-enriched microdomains; TGF- $\beta$ 1, transforming growth factor beta 1; tGFP, turbo green fluorescent protein; TM4SF5, transmembrane 4 L six family member 5; TSAHC, 4'-(*p*-toluenesulfonylamido)-4-hydroxychalcone; Twist-1, Twist-related protein 1; WT, wild type.

Epithelial-mesenchymal transition (EMT), the process by which epithelial cells lose their polarity and gain mesenchymal traits,<sup>4</sup> was shown to generate stem cells in mammary epithelial models.<sup>5</sup> EMT has been suggested to play roles in formation of circulating tumor cells (CTCs), which can eventually form metastatic tumors.<sup>6</sup> Metastatic cells that have undergone EMT are thought to resemble cancer stem cells (CSCs)<sup>7</sup> because they can initiate tumor growth after colonization at a distant region and are enriched for genes associated with stemness as well as drug resistance.<sup>8</sup> Although previous reports suggested that CSCs may arise from transformation of normal cells, more recent reports have suggested that these cells are derived from fully differentiated cells through adaptive transdifferentiation mechanisms, such as EMT.<sup>5</sup> Therefore, CTCs may acquire self-renewal capacity during cancer metastasis.<sup>9</sup> However, the molecules responsible for acquisitions of these CTC characteristics are not fully known.

As a tetraspan(in), transmembrane 4 L six family member 5 (TM4SF5) is highly expressed in diverse cancers, such as HCC, induces EMT, and collaborates with integrins,<sup>10</sup> resulting in morphological elongation through actin reorganization.<sup>11</sup> Moreover, gefitinib resistance in non-small-cell lung cancer depends on TM4SF5-mediated EMT.<sup>12</sup>

Because TM4SF5 induces EMT, we hypothesized that TM4SF5 may be involved in generating CTC phenotypes in HCC. Here, using *in vitro* cells and an *in vivo* animal system, we observed an interaction between TM4SF5 and CD44 that conferred self-renewal properties through the signaling pathway

involving proto-oncogene tyrosine-protein kinase Src (c-Src), signal transducer and activator of transcription 3 (STAT3), Twist-related protein 1 (Twist1), and B-cell-specific Moloney murine leukemia virus integration site 1 (Bmi1), leading to the presence of TM4SF5-dependent metastatic CTCs in the blood.

## Materials and Methods

**Cells.** HCC cells, including SNU449 cells expressing WT TM4SF5 (SNU449Tp pooled clone, T<sub>3</sub>, T<sub>7</sub>, T<sub>10</sub>, and T<sub>16</sub> single-cell-derived clones), *N*-glycosylation mutants of TM4SF5 (N138A, N155Q, or N138A/N155Q [NANQ]), or no TM4SF5 (SNU449 parental [P] or the Cp negative pooled clone), were previously described.<sup>11</sup> Huh7 cells endogenously or SNU449T<sub>7</sub> clone exogenously expressing TM4SF5 were stably transfected with a scrambled control short hairpin RNA (shRNA; turbo green fluorescent protein [tGFP)-shScram in pGFP-V-RS plasmid; OriGene, Rockville, MD) or shRNA against TM4SF5<sup>13</sup> (tGFP-shTM4SF5 in pGFP-V-RS plasmid, catalog no.: TG308787; OriGene). SNU449 and SNU761 cells did not express detectable levels of TM4SF5, whereas Huh7 and HepG2 cells express TM4SF5.<sup>14</sup> SNU449T<sub>7</sub> cells were also stably transfected with shRNA against CD44 (Addgene, Cambridge, MA). Cells were maintained in RPMI-1640 medium (Wel-Gene, Daegu, Korea) containing 10% fetal bovine serum (FBS) and 1% penicillin/streptomycin (GenDEPOT Inc., Barker, TX).

**Spheroid Formation Assay.** Cells were collected, washed twice with phosphate-buffered saline (PBS) to

---

From the <sup>1</sup>Department of Pharmacy, College of Pharmacy, Research Institute of Pharmaceutical Sciences, Seoul National University, Seoul, Korea; <sup>2</sup>Department of Nuclear Medicine, Cancer Research Institute, College of Medicine, Seoul National University, Seoul, Korea; <sup>3</sup>Interdisciplinary Program in Genetic Engineering, Seoul National University, Seoul, Korea; <sup>4</sup>Department of Biomedical Sciences, College of Medicine, Seoul National University, Seoul, Korea; <sup>5</sup>Cancer Imaging Center, Seoul National University Hospital, Seoul, Korea; <sup>6</sup>Division of Applied Life Science, Gyeongsang National University, Jinju, Korea; <sup>7</sup>School of Life Sciences and Biotechnology, Korea University, Seoul, Korea; <sup>8</sup>Graduate School of Nanoscience and Technology, Korea Advanced Institute of Science and Technology, Daejeon, Korea

Received October 9, 2014; accepted January 21, 2015.

Additional Supporting Information may be found at [onlinelibrary.wiley.com/doi/10.1002/hep.27721/supinfo](http://onlinelibrary.wiley.com/doi/10.1002/hep.27721/supinfo)

This work was supported by a grant of the Korea Health Technology R&D Project through the KHIDI, Republic of Korea (HI14C1072; to H.Y.), and by the NRF of Korea grant for the Tumor Microenvironment GCRC funded by the Korea Ministry of Science, ICT & Future Planning (2011-0030001; to H.Y. and J.W.L.), for senior Leap research (2012-0005606/2013-035235), and for Medicinal Bioconvergence Research Center (NRF-2012M3A6A4054271; to J.W.L.).

\*These authors contributed equally.

Address reprint requests to: Jung Weon Lee, Ph.D., Department of Pharmacy, College of Pharmacy, Seoul National University, Seoul 151-742, Korea. E-mail: [jwl@snu.ac.kr](mailto:jwl@snu.ac.kr); fax: +8228721795.

Copyright © 2015 by the American Association for the Study of Liver Diseases.

View this article online at [wileyonlinelibrary.com](http://wileyonlinelibrary.com).

DOI 10.1002/hep.27721

Potential conflict of interest: Nothing to report.

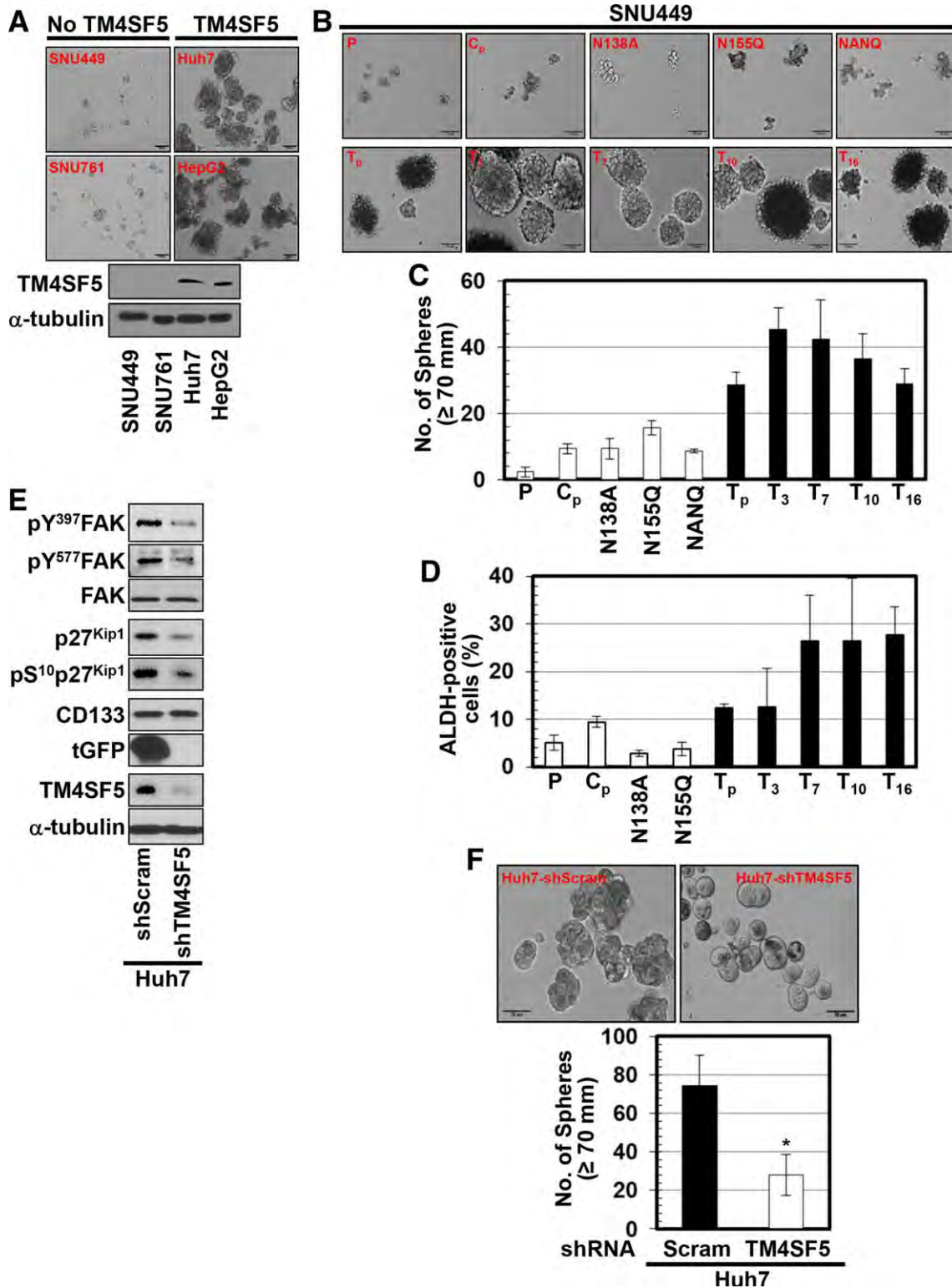


Fig. 1. TM4SF5 expression promoted spheroid formation in HCC. (A-C) Spheroid formation assays showed that TM4SF5-expressing cells (Huh7, HepG2 [A], SNU449<sub>T<sub>p</sub></sub>, SNU449<sub>T<sub>3</sub></sub>, SNU449<sub>T<sub>7</sub></sub>, SNU449<sub>T<sub>10</sub></sub>, and SNU449<sub>T<sub>16</sub></sub> clones [B]) exhibited enhanced sphere-forming capacities, compared to cells lacking TM4SF5 (SNU449 parental, P, and SNU449C<sub>p</sub> stable clone) or expressing the N-glycosylation TM4SF5 mutant (N138A, N155Q, and NANQ [N138A/N155Q]). Images were saved 10 days after seeding cells into six-well ultralow attachment plates. Scale bars represent 70 μm (B). Spheroids larger than 70 μm were selected by sieving and counting (C). (D) ALDEFLUOR assays were performed using spheroids larger than 70 μm. (E and F) Stable knockdown of endogenous TM4SF5 in Huh7 cells was done before analyses of spheroid formation (E) and TM4SF5-mediated downstream signaling activities (F). \*P < 0.05 for a statistical significance. Graphs show the spheroid numbers (C and F) or ALDH activity (D) at the mean ± standard deviation. All data are representative of three independent experiments.

remove serum, and then suspended in serum-free Dulbecco's modified eagle's medium/F12 media supplemented with 1% penicillin/streptomycin (GenDEPOT Inc.) and 2% B27 supplement (Invitrogen, Grand Island, NY). Human epidermal growth factor (EGF) and basic fibroblast growth factor (25 ng/mL; Pepro-Tech, Rocky Hill, NJ) were added to culture every other day. Cells were subsequently cultured in ultralow attachment six-well plates (Corning Inc., Corning, NY) at a density of no more than  $5 \times 10^3$  cells/well with or without specific inhibitors against TM4SF5 (20  $\mu$ M of TSAHC<sup>15</sup>), c-Src (20  $\mu$ M of PP2; LC Labs, Woburn, MA), or STAT3 (1~4  $\mu$ M of STATtics). Representative spheroid images were photographed using a microscope (CKX41; Olympus, Tokyo, Japan) or a time-lapse IX81-ZDC microscope (Olympus).

**Western Blottings.** Spheroids or subconfluent cells in media containing 10% FBS were harvested as whole-cell lysates using a modified radioimmunoprecipitation assay lysis buffer containing 0.1% sodium dodecyl sulfate, 0.5% deoxycholate, 1% nonyl phenoxypolyethoxyethanol, and proteinase inhibitors.<sup>11</sup> Tissue extracts from human or mouse livers were also prepared, as previously described.<sup>11</sup>

**Flow Cytometry.** Stable SNU449 cell clones with or without 4'-p-toluenesulfonylamido)-4-hydroxychalcone (TSAHC) treatment, cells prepared from primary or secondary xenograft tumors, and cells sorted from blood samples were processed for fluorescence-activated cell sorting (FACS) analysis, as previously described.<sup>16</sup>

**Analyses of Mouse or Human Tissues.** All procedures using animal and human tissues were performed in accordance with the procedures of the Seoul National University Institutional Review Board (Seoul, Korea) agreement.

**Statistical Analyses.** Student *t* tests were performed for statistical comparisons of mean values. A *P* value less than 0.05 was considered statistically significance.

**Supporting Information.** Supporting figures and Supporting Information on cell culture, drug sensitivity, reverse-transcription polymerase chain reaction (RT-PCR), western blottings, coimmunoprecipitations, ALDERFLUOR assay, flow cytometry (FCM), serial mouse xenografts, immunohistochemistry (IHC) of mouse or human tissues, and orthotopic tumor cell injection and blood collection for CTC identification can be found at the journal website.

## Results

Ectopic TM4SF5 expression in SNU449 HCC cells was associated with loss of cell-cell adhesion molecule

expression, as well as concomitant induction of mesenchymal markers (Supporting Fig. 1A). Furthermore, knockdown of endogenous TM4SF5 in Huh7 cells increased the expression of cell-cell adhesion molecules, but decreased mesenchymal markers (Supporting Fig. 1B). Moreover, TM4SF5 expression correlated with the resistance of cells to the anticancer agent, paclitaxel (Supporting Fig. 1C). Because EMT and drug resistance characteristics were associated with TM4SF5, TM4SF5-mediated self-renewal properties were further explored.

**TM4SF5 Expression Promoted Spheroid Formation in HCC.** We first tested whether TM4SF5 could form spheroids in a low-adhesive environment. Unlike the TM4SF5-null SNU449 and SNU761 HCC cell lines, Huh7 and HepG2 HCC cells with endogenous TM4SF5<sup>14</sup> formed spheroids (Fig. 1A). TM4SF5-expressing SNU449 transfectants (SNU449Tp, pooled clone; T<sub>3</sub>, T<sub>7</sub>, T<sub>10</sub>, and T<sub>16</sub> single-cell-derived clones) readily formed spheroids, whereas the TM4SF5-negative pooled clone (SNU449Cp) and the *N*-glycosylation mutant (N138A, N115Q, or N138A/N155Q) cells did not (Fig. 1B). The number of spheroids larger than 70  $\mu$ m correlated with wild type (WT) TM4SF5 expression (Fig. 1C). Aldehyde dehydrogenase (ALDH) enzyme activities were higher in WT TM4SF5-expressing cells than in TM4SF5-null- or -mutant-expressing cells (Fig. 1D and Supporting Fig. 1D). TM4SF5 knockdown in Huh7 cells exhibited decreased phospho-FAK, p27<sup>Kip1</sup> expression, and phospho-Ser10 p27<sup>Kip1</sup> levels (Fig. 1E), as expected based on a previous study,<sup>11</sup> and formed fewer spheroids (Fig. 1F). TM4SF5 knockdown in stable SNU449T<sub>7</sub> cells also abolished spheroid formation (Supporting Fig. 2). Taken together, the results demonstrated that TM4SF5 was thus involved in spheroid formation.

**TM4SF5 Interacted With CD44 for Spheroid Formation.** We next examined expression levels of molecules that might be associated with self-renewal. *CD24* messenger RNA (mRNA) expression was lower in TM4SF5-positive cells than in TM4SF5-negative cells, whereas *CD44* mRNA expression was similar in both TM4SF5-negative and -positive cells (Fig. 2A). Protein levels showed similar patterns by western blottings and FACS analysis (Fig. 2B-D). The anti-CD44 clone, IM7 (BioLegend, San Diego, CA), revealed similar CD44 expression levels on TM4SF5-negative or -mutant cells and WT TM4SF5-expressing cells (Fig. 2D, upper), whereas the anti-CD44 clone, DF1485 (Santa Cruz Biotechnology, Santa Cruz, CA), showed a positive signal only in TM4SF5-negative or mutant

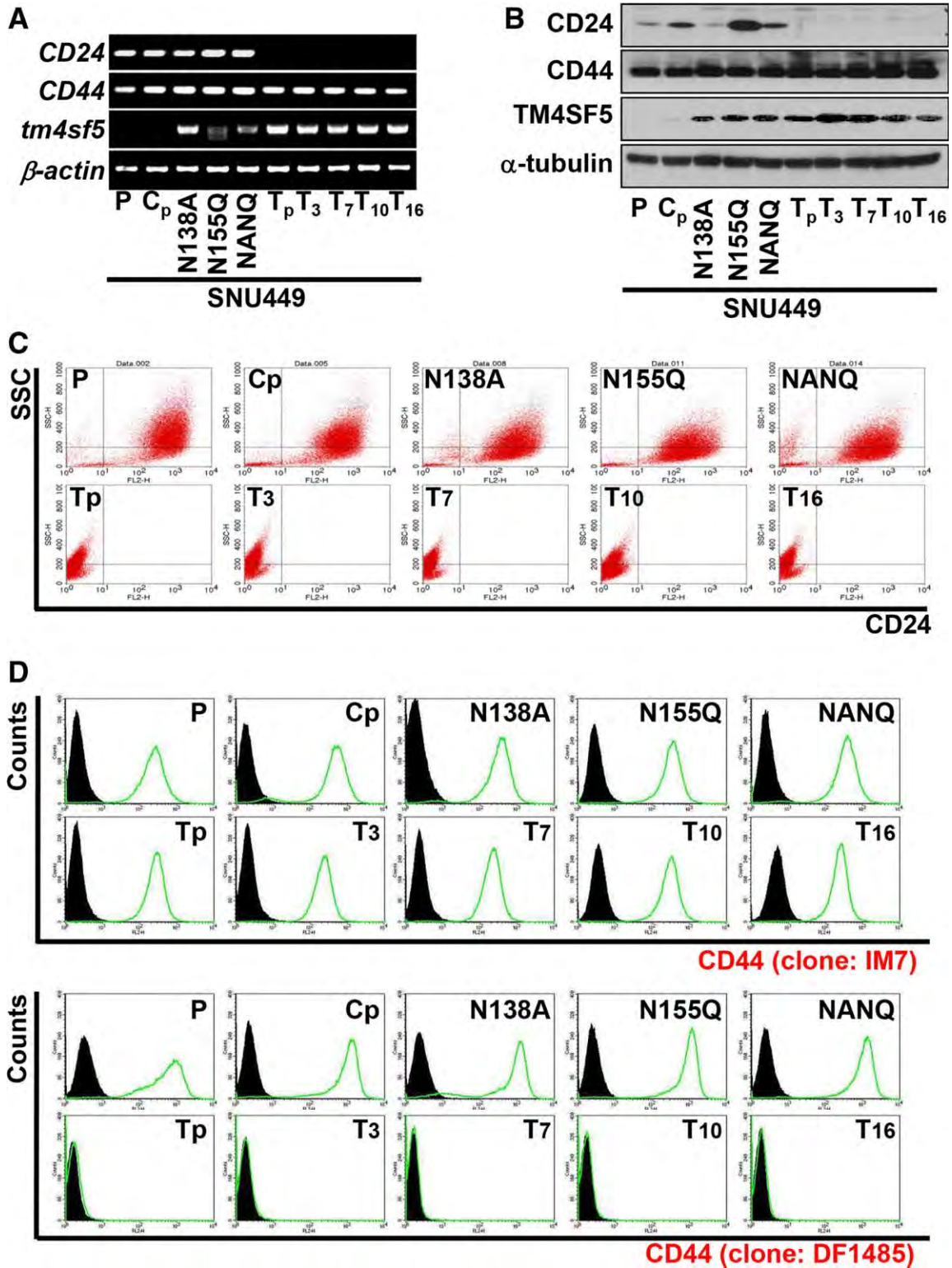


Fig. 2. TM4SF5 and CD44 appeared important for spheroid formation. (A) mRNA levels were determined by RT-PCR from stable SNU449 cell clones.  $\beta$ -actin was used as a control. (B) Whole-cell lysates from cells were immunoblotted for the indicated molecules. (C and D) FCM analysis was performed for CD24 (B) and CD44 (C; upper panel using the anti-CD44 Ab IM7 clone and lower panel using the DF1485 clone) expression in stable SNU449 cell clones. Black histograms indicate no secondary Ab controls. (E) FCM analysis was performed using the anti-CD44 DF1485 clone for CD44 expression in SNU449 stable cell clones after 24-hour DMSO or TSAHC (20  $\mu$ M) treatment. TSAHC- (red) and DMSO-treated cells (green) were compared with no secondary Ab controls (black field). (F) Stable SNU449 clones treated with DMSO or TSAHC (20  $\mu$ M) for 24 hours were processed for RT-PCR to analyze *CD44* and  $\beta$ -actin mRNA levels. Data represent three independent experiments.

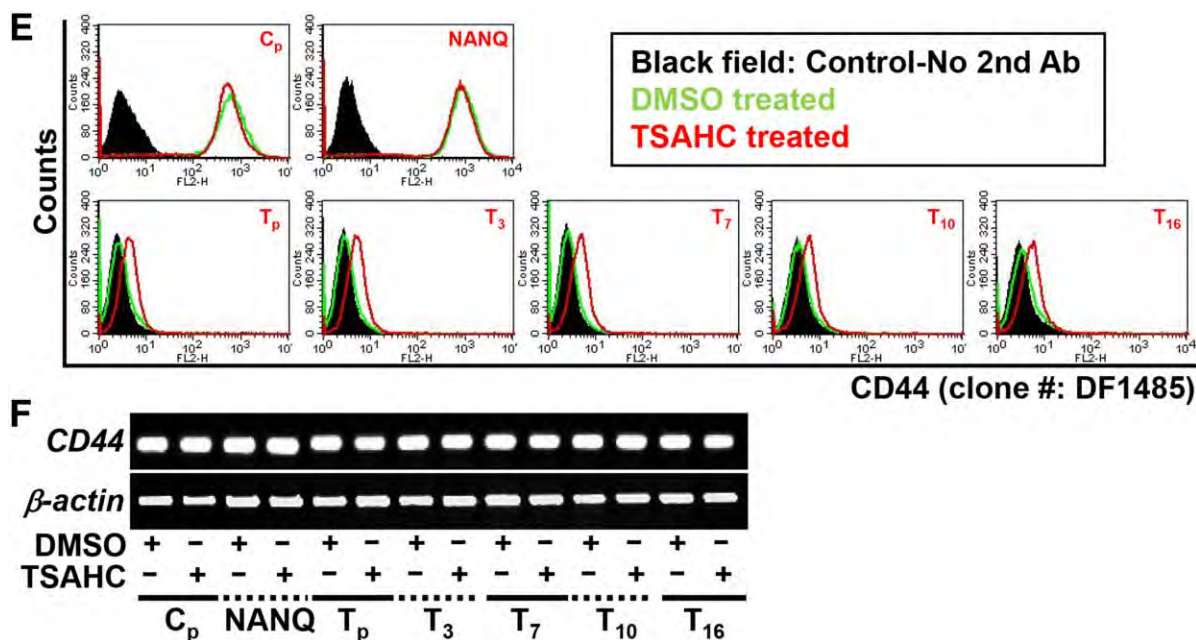


Fig. 2. (Continued)

cells (Fig. 2D, lower). This difference may have been owing to differential epitope availability in CD44, which presumably resulted from a different conformational context owing to TM4SF5 expression and/or interaction. Treatment with the anti-TM4SF5 reagent, TSAHC, which disrupts the *N*-glycosylation pattern of TM4SF5,<sup>15</sup> did not change CD44 levels on TM4SF5-negative or -mutant cells, but slightly increased CD44 levels on WT TM4SF5-expressing cells (Fig. 2E), although TSAHC did not cause additional *CD44* mRNA transcription (Fig. 2F). Furthermore, the WT TM4SF5, but not the *N*-glycosylation mutant, did not coimmunoprecipitate with endogenous CD44 (Fig. 3A). This TM4SF5-CD44 interaction occurred through extracellular domains; the CD44- $\Delta$ <sub>ICD</sub> (deletion mutant without the intracellular domain) was pulled down by STrEP-tagged WT TM4SF5 (Fig. 3B), again depending on TSAHC treatment (Fig. 3C). Knockdown of TM4SF5 also increased the level of CD44 recognized by anti-CD44 DF1485 antibody (Ab; Fig. 3D). Consistently, WT TM4SF5-dependent spheroid formation was abolished by TSAHC treatment (Fig. 3E), as well as by CD44 knockdown (Fig. 3F). Therefore, the physical association between CD44 and TM4SF5 appeared critical for TM4SF5-mediated spheroid formation.

**Self-Renewal Properties Were Controlled by TM4SF5 Expression.** When fewer than 5,000 SNU449Cp (or TM4SF5<sub>N138A/N155Q</sub>) or WT TM4SF5-positive SNU449T<sub>7</sub> cells were subcutaneously injected into left or right flanks of mice,

SNU449T<sub>7</sub> cells clearly formed tumors, whereas control or mutant cells did not (Fig. 4A). Cells purified from the primary xenografts (i.e., ExpT<sub>7-2</sub> cells of mouse 2, ExpT<sub>7-2</sub>) showed similar or greater TM4SF5 expression and TM4SF5 downstream-signaling activities, compared to those in original SNU449T<sub>7</sub> cells (Fig. 4A, middle immunoblotting panel). ExpT<sub>7-2</sub> cells formed more-aggressive spheroids than SNU449T<sub>7</sub> cells (Fig. 4A, bottom spheroid image). ExpT<sub>7-2</sub> or ExpT<sub>7-3</sub> cells formed tumors more aggressively and at cell numbers as low as 200 cells per injection in secondary xenografts (Fig. 4B and Supporting Fig. 3A). Consistently, cells purified from secondary xenografts (i.e., 2<sup>nd</sup>ExpT<sub>7-2</sub>) exhibited a further increase in phospho-c-Src levels, compared with the SNU449Cp, SNU449T<sub>7</sub>, or ExpT<sub>7-2</sub> cells (Fig. 4B, bottom).

Using WT TM4SF5-dependent xenograft tissues, double IHC for TM4SF5 and CD44 showed distinct cell populations with either higher CD44 level (reddish) or both TM4SF5 and CD44 (yellowish) expression levels (Fig. 4C). Thus, SNU449T<sub>7</sub> cells could have differentiated into heterogeneous cell types with varied TM4SF5 and/or CD44 expression levels during xenograft formation. When analyzed by FACS, CD44 (as measured by the IM7 Ab clone) and TM4SF5 were more highly expressed in ExpT<sub>7-2</sub>, ExpT<sub>7-3</sub>, and 2<sup>nd</sup>ExpT<sub>7-2</sub> cells, compared to original SNU449T<sub>7</sub> cells (Fig. 4D and Supporting Fig. 3B). However, surface levels of CD24, CD90, and CD133 were unchanged, suggesting that these markers might not be involved in TM4SF5-mediated effects. Dual labeling

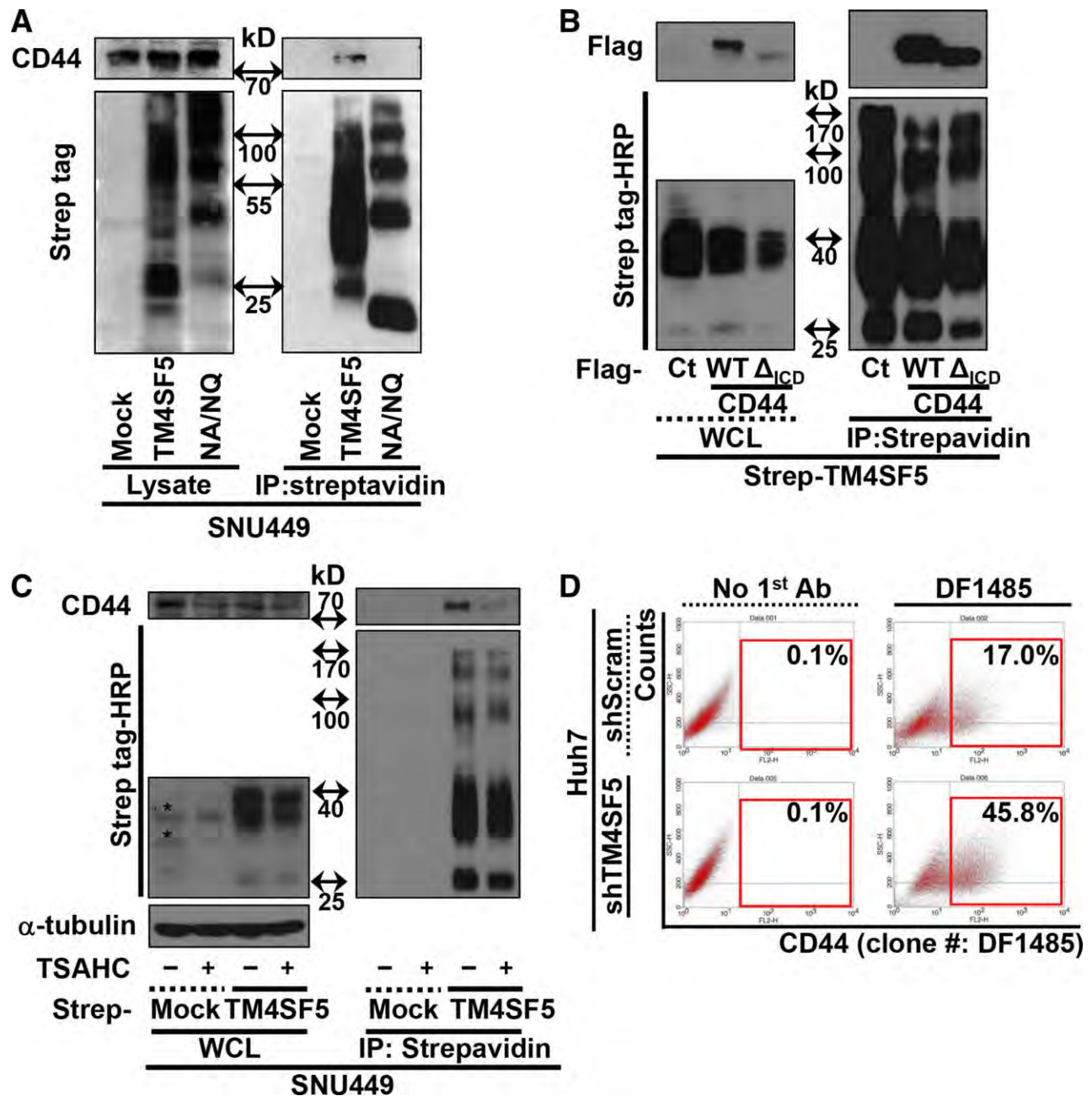


Fig. 3. Spheroid formation depending on the extracellular interaction between TM4SF5 and CD44. (A-C) SNU449 parental cells were transfected with the indicated expression vectors for 48 hours (A and B). DMSO (–) or 20  $\mu$ M of TSAHC (+) was treated for an additional 24 hours (C). Whole-cell lysates were prepared and pulled down using streptavidin beads before standard western blotting. (D) FCM analysis using the DF1485 Ab was performed for CD44 expression in Huh7 cells stably expressing shScramble (upper panels) or shTM4SF5 (lower panels). (E) Stable SNU449 clones (normal) or cells treated with DMSO or TSAHC (20  $\mu$ M) were analyzed for spheroid formation. (F) Stable TM4SF5-expressing SNU449T<sub>7</sub> cells were stably transfected with shRNA against a scramble sequence (shScram) or CD44 (shCD44) before spheroid formation analysis for 10 days. The numbers of spheroids ( $\geq 70$   $\mu$ m) are graphed at the mean  $\pm$  standard deviation. Data represent three independent experiments. Abbreviations: IP:Streptavidin, immunoprecipitated with streptavidin; WCL, whole cell lysate.

of ExpT<sub>7-2</sub> or ExpT<sub>7-3</sub> produced histograms showing populations with either increased expression of CD44 or TM4SF5, or an increase in both markers (Fig. 4E).

**TM4SF5 Regulates *c-Src*, *STAT3*, *Twist1*, and *Bmi1* for Self-Renewal Properties.** Phospho-Tyr416 *c-Src*, phospho-Tyr705 *STAT3*, *Twist1* mRNA, and

*Bmi1* mRNA levels correlated with TM4SF5-mediated spheroid formation (Fig. 5A). Knockdown of either TM4SF5 or CD44 in SNU449T<sub>7</sub> cells reduced their levels and negatively affected phosphorylation of focal adhesion kinase (FAK) and p27<sup>Kip1</sup> downstream of TM4SF5.<sup>11</sup> However, CD44 knockdown did not reduce phospho-Ser10 p27<sup>Kip1</sup> (Fig.

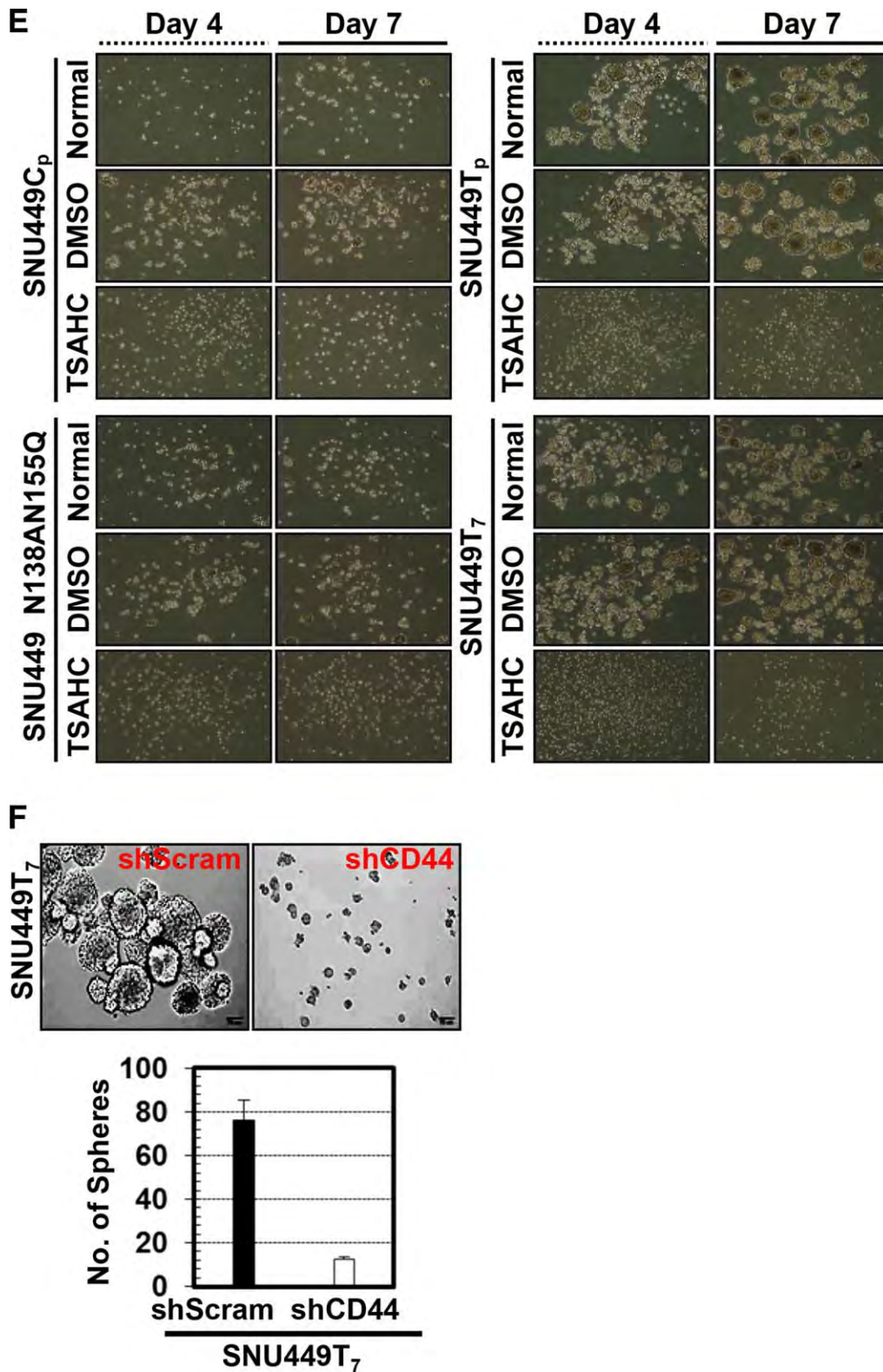


Fig. 3. (Continued)

5B,C). Furthermore, xenografts formed from SNU449T<sub>7</sub> cells (mice 2 and 3) exhibited coexpression of CD44 and Bmi1 within TM4SF5-positive areas (Fig. 5D).

Treatment of TM4SF5-expressing cell clones with TSAHC decreased levels of phospho-Tyr416 c-Src, phospho-Tyr705 STAT3, Twist1, and *Bmi1* mRNA (Fig. 5E). As TSAHC treatment of Huh7 cells

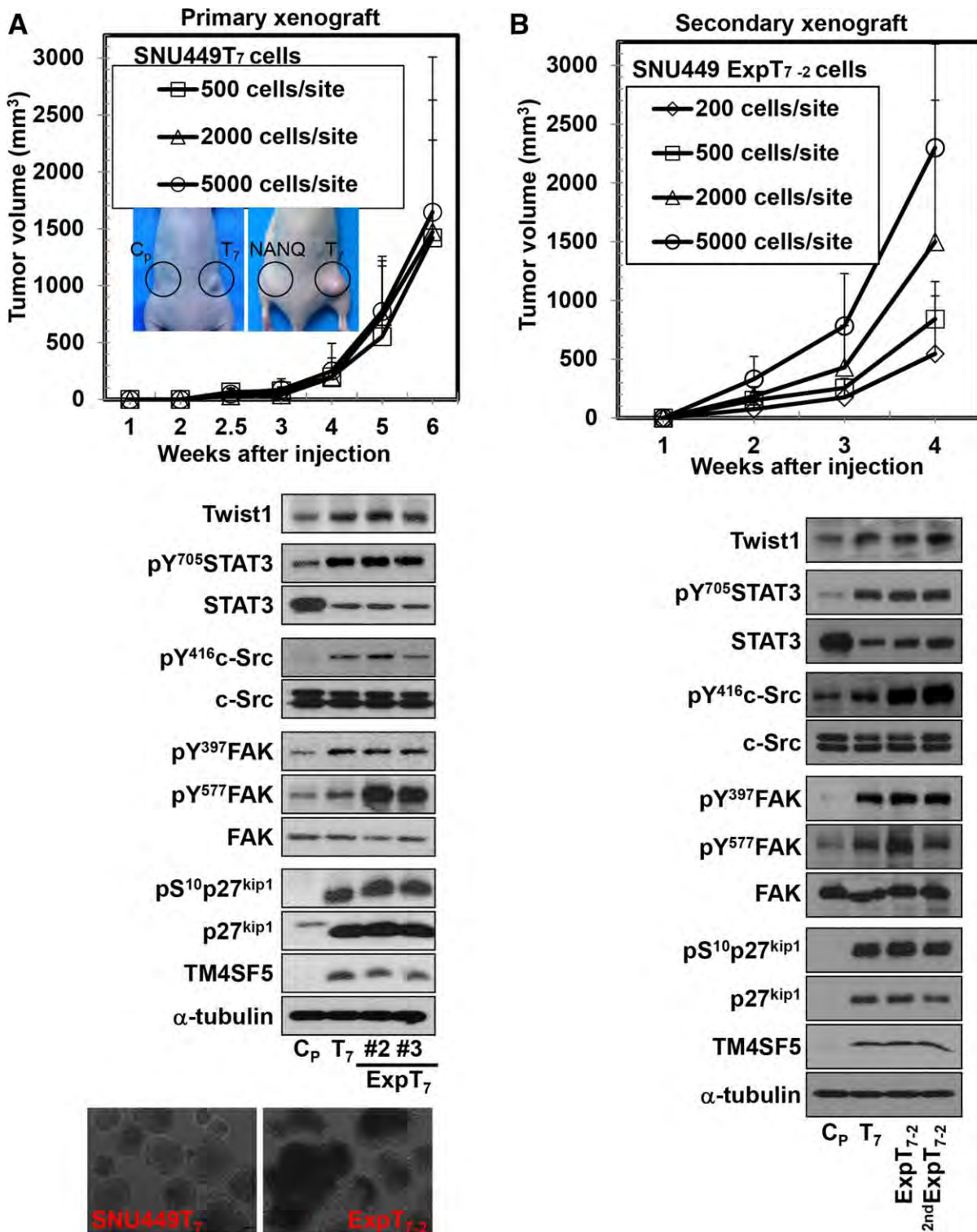


Fig. 4. Self-renewal properties were controlled by TM4SF5 expression (A; top graph and images). Representative images (inserts) showing tumors formed by subcutaneous injection of stable SNU449 cell clones (TM4SF5-null SNU449C<sub>p</sub>; C<sub>p</sub> [n = 5], TM4SF5 N138A/N155Q mutant-expressing SNU449 clone; NANQ [n = 5], T<sub>7</sub>; and TM4SF5-expressing SNU449T<sub>7</sub> cells [n = 10]) using less than 5,000 cells per injection site. Tumors were formed only in SNU449T<sub>7</sub> cell-injected flanks, as shown in graphs of different cell numbers per injection site. TM4SF5-null or -mutant cells are not shown owing to no tumor formation. Tumor volumes are reported as mean ± standard deviation values for each number of SNU449T<sub>7</sub> cells injected. (A; middle immunoblots) SNU449C<sub>p</sub> (C<sub>p</sub>), SNU449T<sub>7</sub>, or ExpT<sub>7</sub> cells (prepared from xenograft tissues [mice 2 and 3]) were harvested for standard western blotting (middle). (A, bottom spheroid images) Spheroid formation was compared for SNU449T<sub>7</sub> and ExpT<sub>7-2</sub> for 10 days (bottom). (B, top graph) Tumor volumes (n = 7) resulting from the subcutaneous injection of ExpT<sub>7-2</sub> (i.e., cells prepared from xenograft tumors after SNU449T<sub>7</sub> cell injection), as shown in graphs at different cell numbers per injection site. TM4SF5-null or -mutant cells are not shown owing to no tumor formation. Tumor volumes are reported as mean ± standard deviation values. (B, bottom immunoblots) SNU449C<sub>p</sub> (C<sub>p</sub>), SNU449T<sub>7</sub> (T<sub>7</sub>), ExpT<sub>7-2</sub>, and secondary explants (2<sup>nd</sup>ExpT<sub>7-2</sub>, cells prepared from xenograft tumors after ExpT<sub>7-2</sub> cell injection) were harvested for standard western blotting. (C) Primary xenograft tumor sections after injection of SNU449T<sub>7</sub> were stained with DAPI (blue) and immunostained for CD44 (red) and TM4SF5 (green). Regions from 3 different mice are shown with enlargement at right. (D) FACS analysis using SNU449T<sub>7</sub>, ExpT<sub>7-2</sub>, and ExpT<sub>7-3</sub> cells was performed for CD44 (using clone IM7 Ab), TM4SF5, CD24, CD90, and CD133. (E) FACS analysis with double staining (with anti-CD44 clone IM7 and anti-TM4SF5<sup>42</sup> Ab) was performed for indicated cells. Data shown represent three independent experiments.

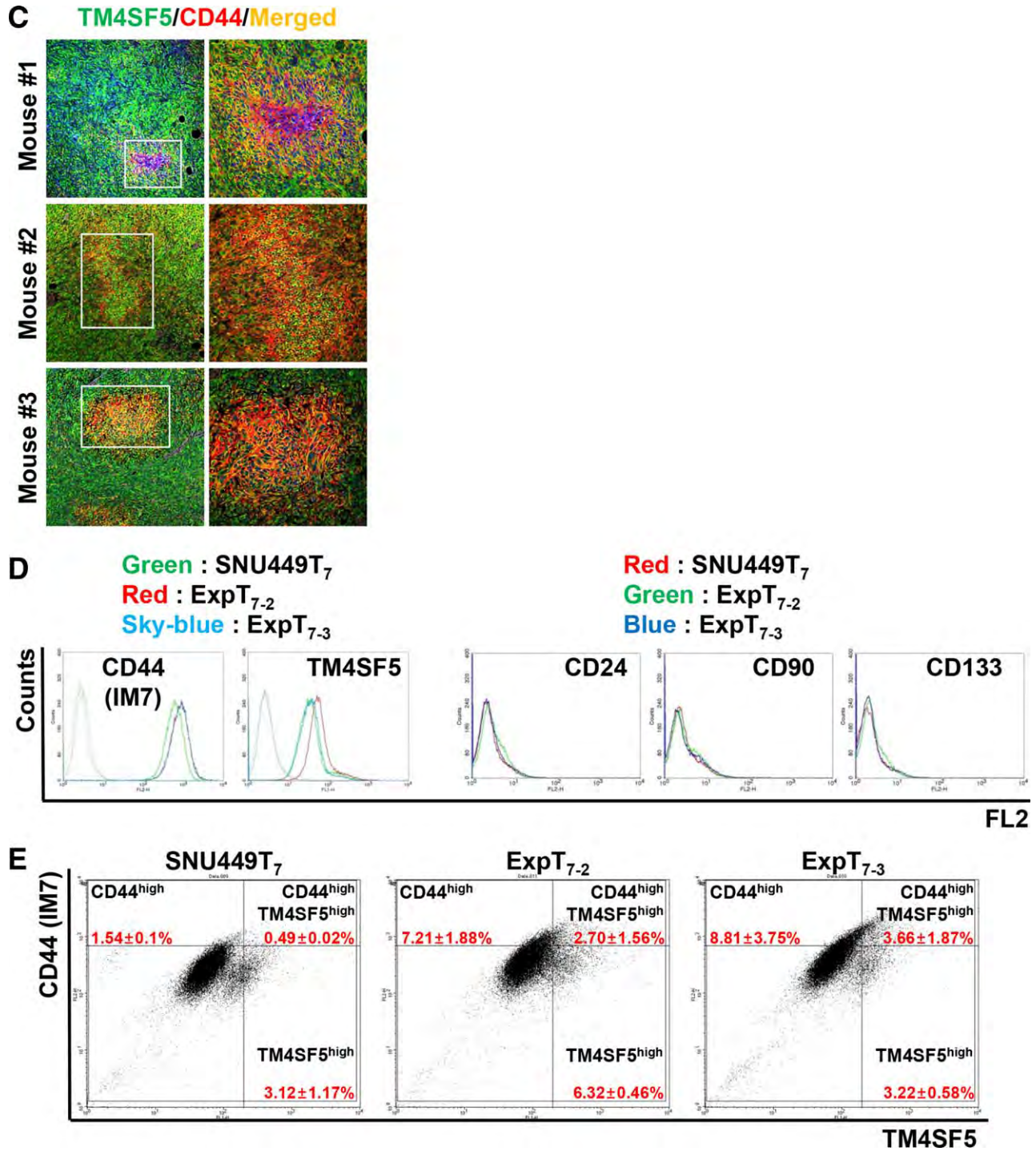


Fig. 4. (Continued)

abolished spheroid formation (Fig. 5E, top), TSAHC decreased TM4SF5-mediated signaling levels and *Bmi1* mRNA levels, compared with dimethyl sulfoxide (DMSO) treatment (Fig. 5E, bottom). Treatment of WT TM4SF5-expressing SNU449T<sub>7</sub> cells with PP2 (but not the control PP3) blocked TM4SF5-dependent spheroid formation (Fig. 6A). Treatment of SNU449T<sub>7</sub> cells with a STAT3 inhibitor (STATic)

abolished spheroid formation (Fig. 6B). After c-Src or STAT3 inhibition, phospho-Tyr705 STAT3 and Twist1 expression decreased, although caspase-3 activation was not observed (Supporting Fig. 4), suggesting that c-Src acted upstream of STAT3, which again acted upstream of Twist1.

Overexpression of *Bmi1* into TM4SF5-null or -mutant (NANQ) cell clones was sufficient to promote

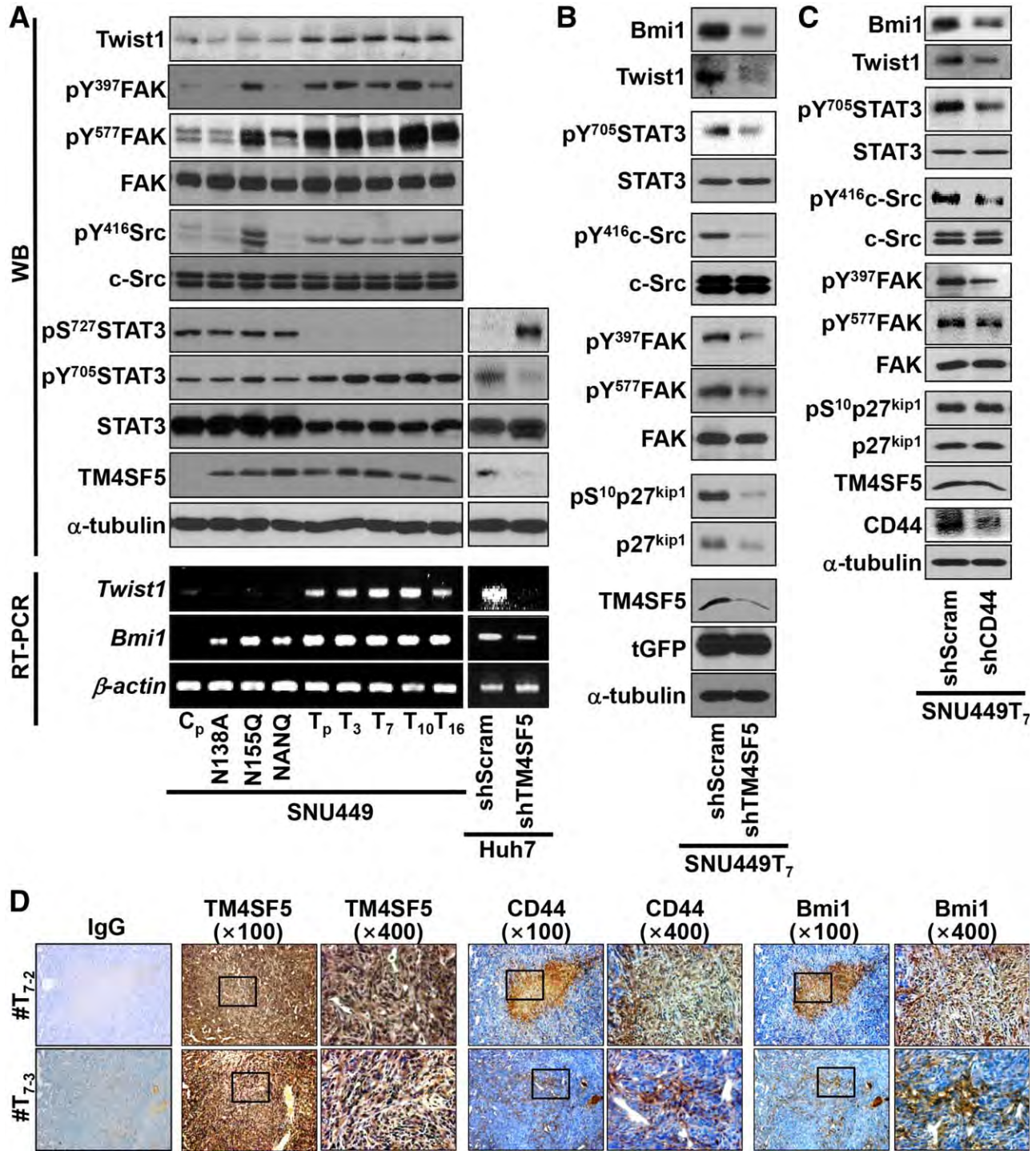


Fig. 5. TM4SF5 regulated c-Src, STAT3, Twist1, and Bmi1 for the self-renewal property. (A) Stable cells were harvested for standard western blotting or processed for RT-PCR. (B and C) SNU449T<sub>7</sub> cells stably transfected with shScram, shTM4SF5, or shCD44 were harvested as whole-cells lysates before standard western blotting. (D) Serial sections (6 μm) from xenograft tissues injected with SNU449T<sub>7</sub> (mice 2 and 3) were immunostained for the molecules. Magnifications, ×100 and ×400. (E) Stable cells expressing TM4SF5 were treated with DMSO or TSAHC (20 μM) for 24 hours, then harvested as whole-cell extracts before standard western blotting or RT-PCR analysis. (F) Huh7 cells (normal) or cells treated with DMSO or TSAHC (20 μM) were examined for spheroid formation (top), then harvested for standard western blotting or RT-PCR (bottom). Data represent three different experiments. Abbreviations: IgG, immunoglobulin G; WB, western blotting.

spheroid formation (Fig. 6C). Meanwhile, knockdown of Bmi1 in SNU449T<sub>7</sub> cells blocked spheroid formation (Fig. 6D). Thus, TM4SF5 required Bmi1 expres-

sion for spheroid formation. Immunostaining of HCC tumor tissue revealed colocalization of TM4SF5 and Bmi1 with local CD44 expression (Fig. 6E), similar to

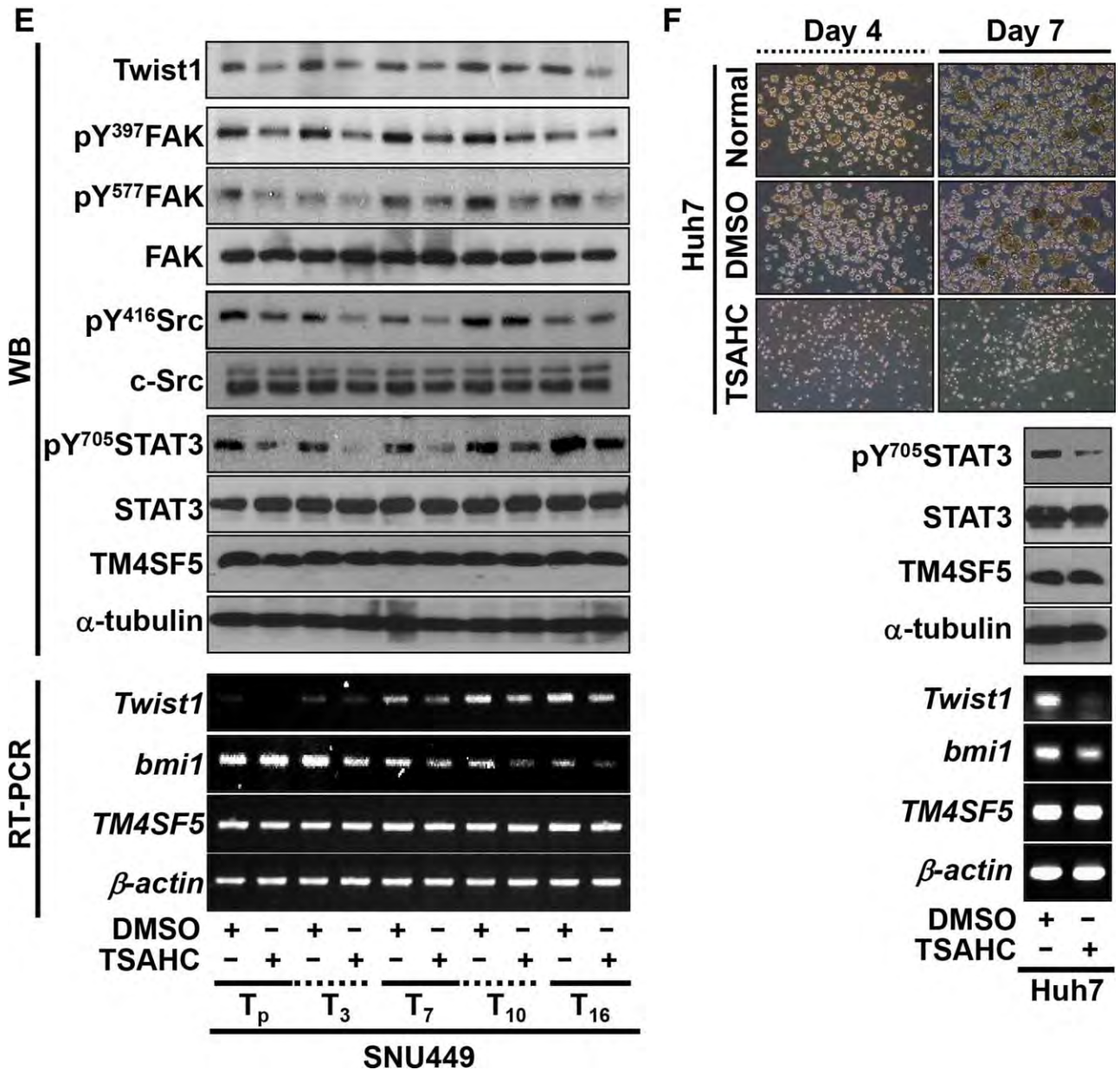


Fig. 5. (Continued)

the results obtained for mouse xenografts (Figs. 4C and 5D). In addition, the Oncomine database revealed that TM4SF5 expression in liver cancer tissues significantly correlates with Bmi1 expression (Supporting Fig. 5).

**Identification of TM4SF5-Dependent CTCs and Their Metastasis.** SNU449T<sub>7</sub> cells stably transfected with tGFP-tagged shRNA constructs against a scrambled sequence (tGFP-shScram) or TM4SF5 (tGFP-shTM4SF5) or the PBS vehicle alone were injected orthotopically into mouse livers. Four or 6 weeks later, blood samples were collected and assayed by anti-tGFP and 4',6-diamidino-2-phenylindole (DAPI) staining. No cells were found in blood samples

of mice injected with PBS or SNU449T<sub>7</sub>-(tGFP)-shTM4SF5 cells, whereas TM4SF5-positive cells were found in mice injected with SNU449T<sub>7</sub>-(tGFP)-shScram cells (Fig. 7A,B). The tGFP signal was also examined in live mice using confocal laser endomicroscopy. When 0.453-mm<sup>3</sup> sections of blood vessels were analyzed for 20 minutes, 2 of 3 SNU449T<sub>7</sub>-(tGFP)-shScram mice exhibited streaming tGFP-positive cells (Fig. 7C), whereas none of the SNU449T<sub>7</sub>-(tGFP)-shTM4SF5 mice showed positive cells (data not shown). After endomicroscopic imaging, blood samples from mice injected with SNU449T<sub>7</sub>-(tGFP)-shScram cells contained green fluorescent cells (Supporting Fig. 6). Furthermore, SNU449T<sub>7</sub>-shControl cells that were

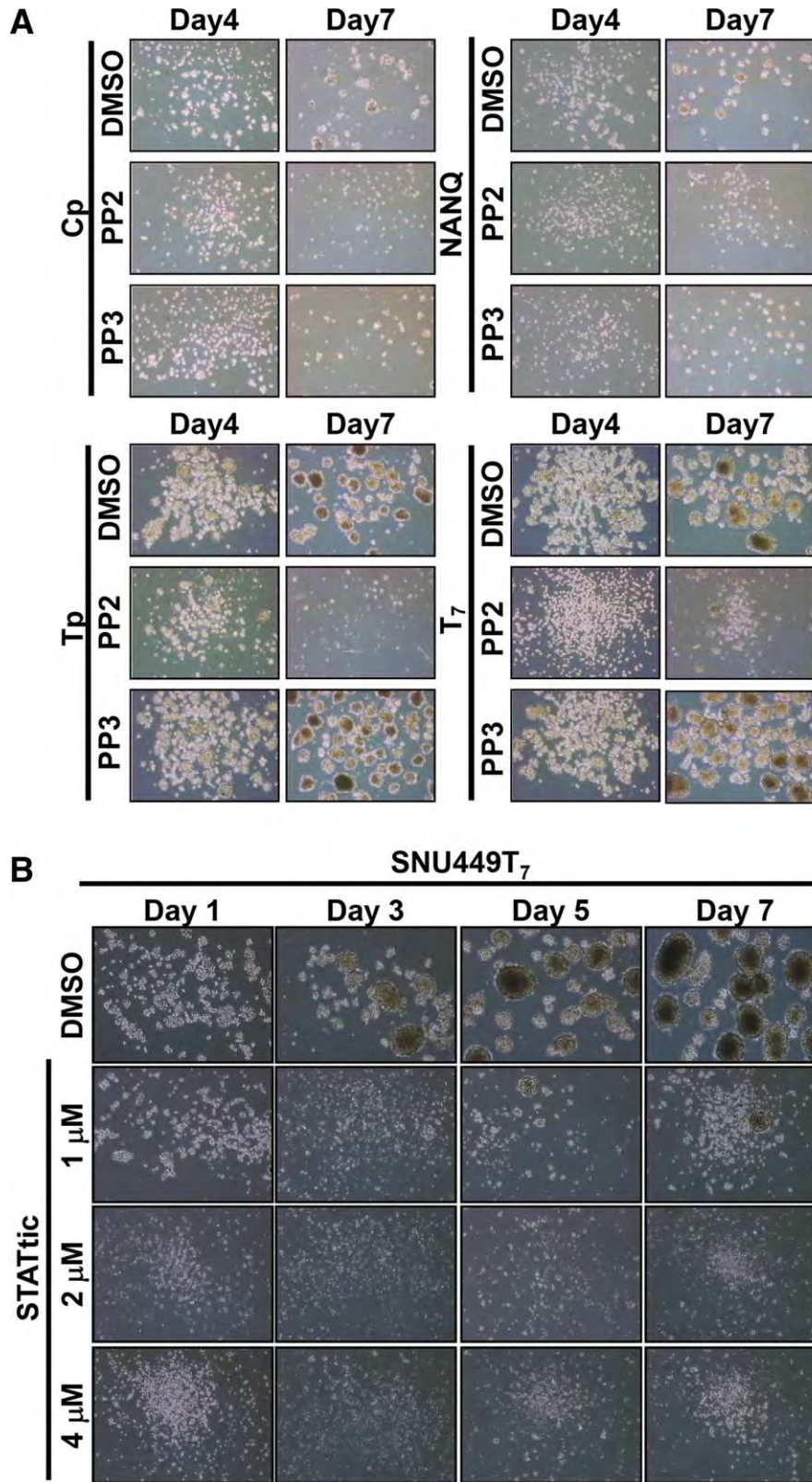


Fig. 6. TM4SF5-dependent c-Src, STAT3, and Bmi1 signaling was required for the self-renewal property. (A and B) Spheroid formation was evaluated in stable SNU449 clones treated with either DMSO, specific c-Src inhibitor PP2, or negative control compound PP3 (A) or treated with either DMSO or STAT3 inhibitor (STATtic) at various concentrations (B). (C and D) Cells were transiently transfected with Bmi1 expression vector (C) or shRNA against Bmi1 (shBmi1; D) for 48 hours and enriched under a selective pressure using G418 (250 μg/mL) for 1 week before western blotting or spheroid forming assays. (E) Serial sections of tumor tissues from clinical HCC patients were processed for IHC using normal mouse or rabbit IgG, TM4SF5, CD44, or Bmi1 Ab. Black boxes indicate the enlarged areas that are shown directly below. Magnifications, ×100 and ×400. Data represent three different experiments. Abbreviation: IgG, immunoglobulin G.

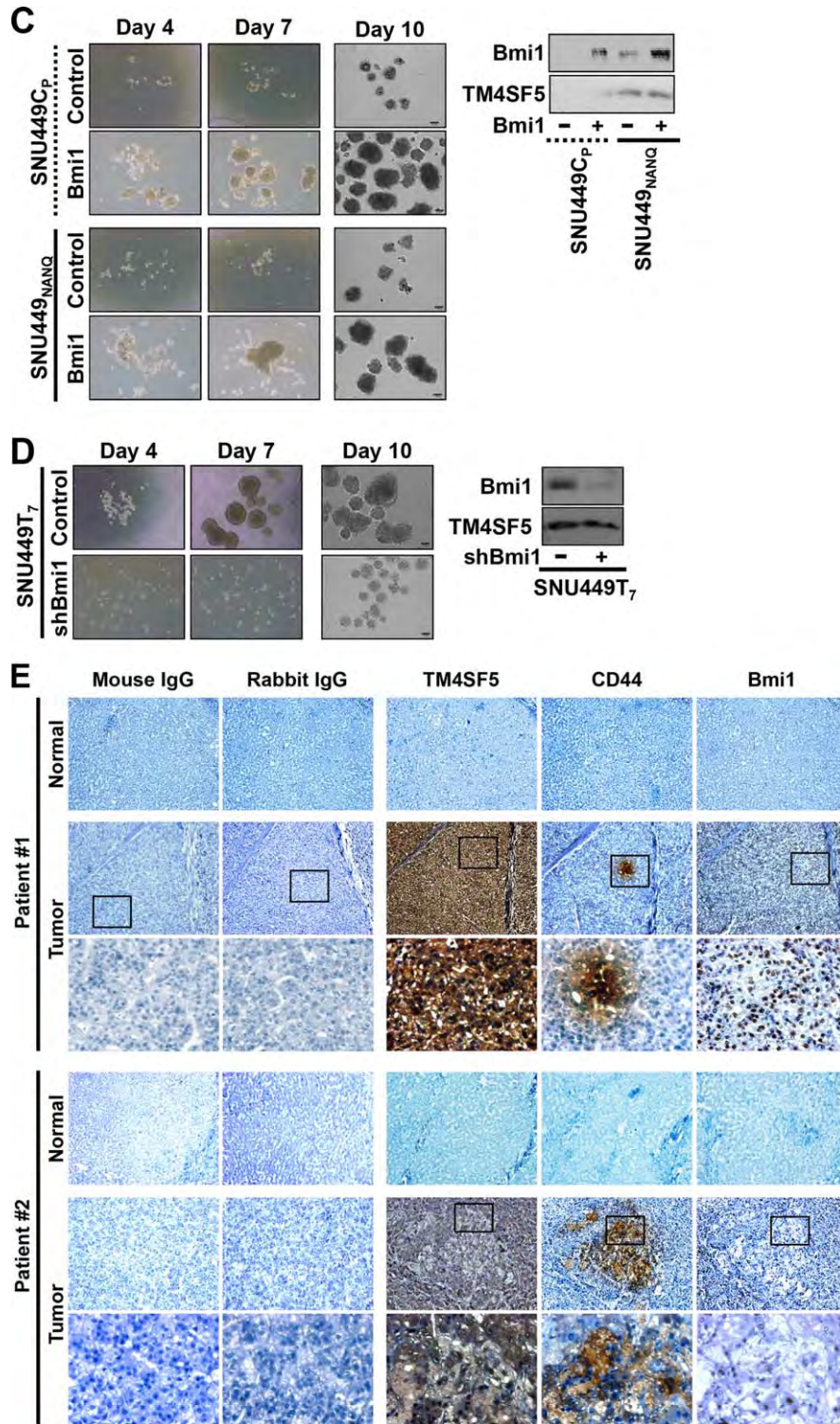


Fig. 6. (Continued)

orthotopically injected into livers were recovered as DAPI-positive cells in blood samples, whereas no such positive cells were observed in blood from mice injected with PBS or SNU449T<sub>7</sub>-shCD44 cells (Fig. 7D). SNU449T<sub>7</sub>-shScramble cell-injected mice exhibited shorter lifespans, whereas PBS-injected or

SNU449T<sub>7</sub>-shCD44 cell-injected mice survived (Fig. 7D).

Orthotopic liver injection of SNU449T<sub>7</sub>-shControl cells after incision was followed by treatment with either DMSO or TSAHC. Whereas DMSO-treated mice showed metastatic cell settlements distal from

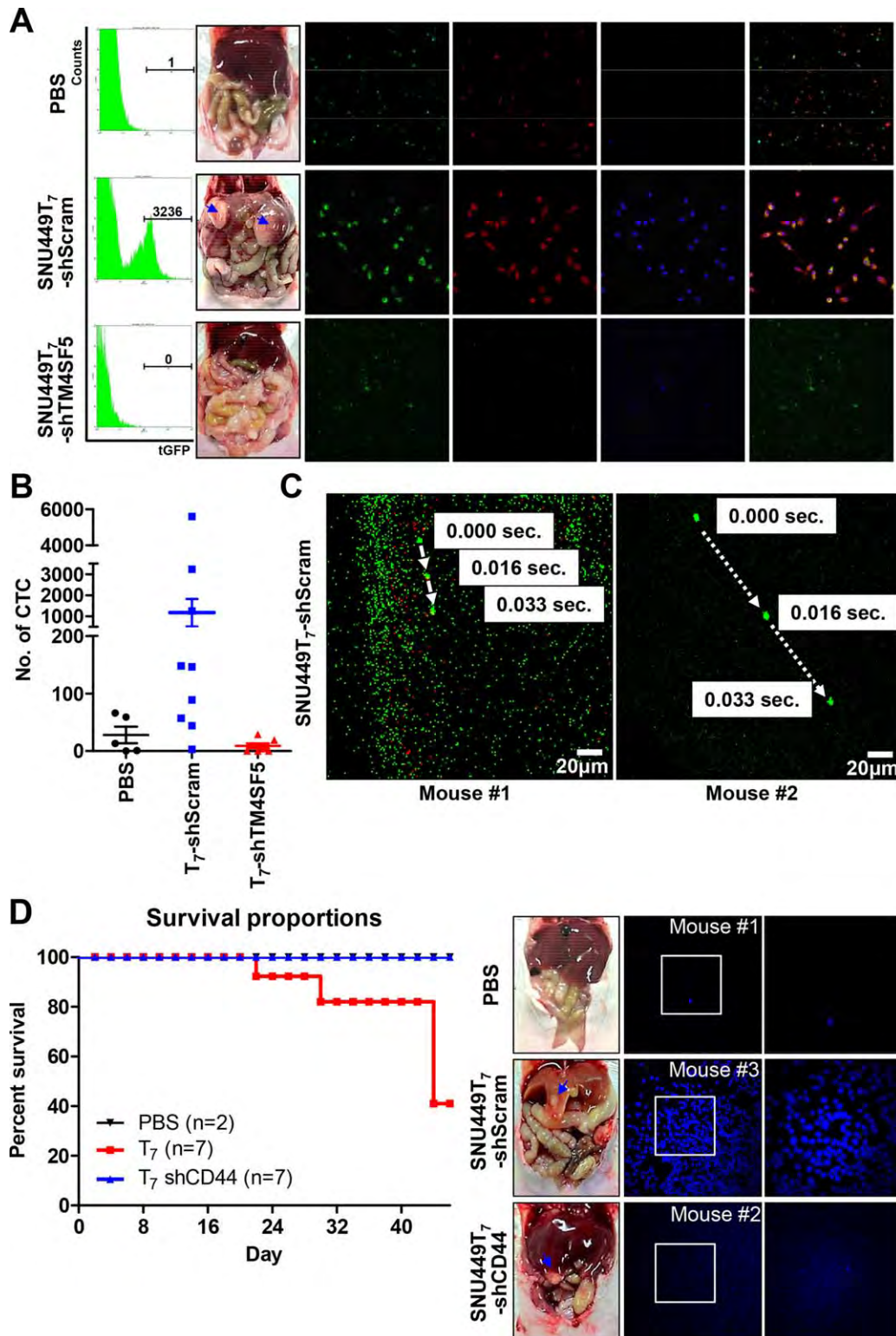


Fig. 7. Identification of TM4SF5-dependent CTCs and their metastasis. SNU449T<sub>7</sub> cells stably transfected with tGFP-shScram or tGFP-shTM4SF5 were orthotopically injected into livers (500,000 cells/mouse for 4 weeks or 200,000 cells/mouse for 6 weeks); separate injections of PBS alone were also performed as controls. (A) Four weeks later, blood samples collected from each mouse (middle images) were processed for FACS sorting (left histograms) and then seeded onto fibronectin-coated (10 µg/mL) coverslips before visualizing for tGFP (green) and staining with anti-tGFP Ab (red) or DAPI (blue). (B) Numbers of CTC-like cells sorted from blood samples of mice injected with PBS (n = 5) were graphed at the mean ± standard deviation, using SNU449T<sub>7</sub>-tGFP-shScram cells (n = 10) or SNU449T<sub>7</sub>-tGFP-shTM4SF5 cells (n = 5). (C) Mice orthotopically injected with SNU449T<sub>7</sub>-tGFP-shScram (n = 3) or SNU449T<sub>7</sub>-tGFP-shTM4SF5 (n = 3) were processed for CTC imaging using confocal laser endomicroscopy 6 weeks after injection. Sections of blood vessels (0.453 mm<sup>2</sup>) from each mouse were imaged for 20 minutes. (D) Mice orthotopically injected with vehicle (PBS; n = 2), SNU449T<sub>7</sub>-shScram cells (n = 7), or SNU449T<sub>7</sub>-shCD44 cells (n = 7) for 6 weeks were processed for collection of blood samples and analysis of survival, then blood samples were processed and visualized using a fluorescent microscope after DAPI staining. Data represent three independent experiments.

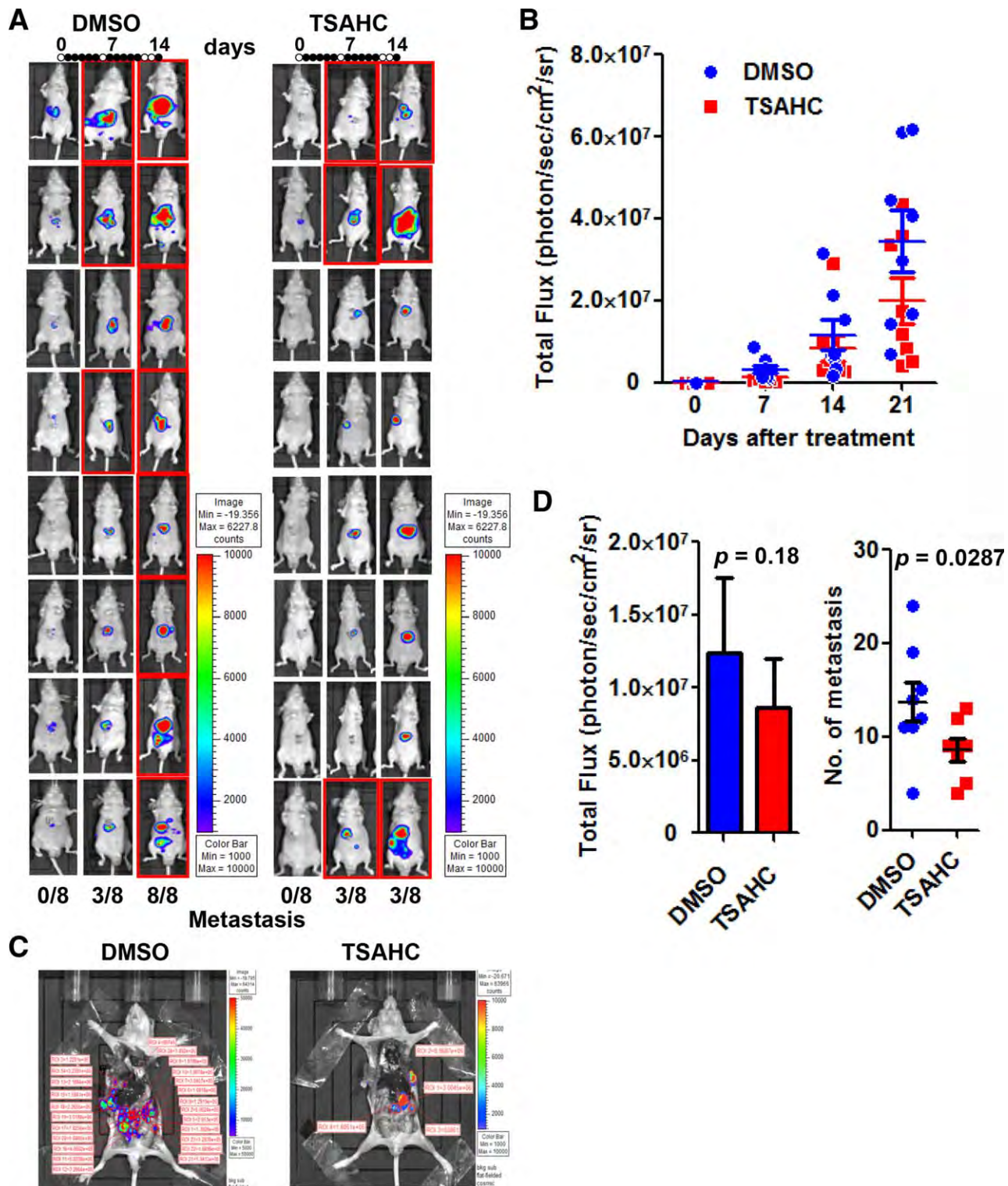


Fig. 8. Anti-TM4SF5 reagent blocked metastasis of orthotopically liver-injected cells to intestines. (A-E) Mice orthotopically liver injected with SNU449T<sub>7</sub>-pMSCV-Luc2 cells were treated with either DMSO or TSAHC, as explained in Materials and Methods. (A) Up to 2 weeks after cell injection and treatment, bioluminescence images were saved. Mice marked with red rectangles depict mice with metastasized tumors. Total bioluminescence flux after 3-week treatment were measured and shown as the mean  $\pm$  standard deviation. (C) Representative images of tumors in mouse treated with DMSO or TSAHC for 3 weeks. (D) Total flux (left) or number of metastatic tumors (right) was measured and presented as the mean  $\pm$  standard deviation.  $P \geq 0.05$  or  $P < 0.05$  depicts statistical insignificance or significance, respectively. (E) Orthotopic tumors or metastatic tumors at the intestine or peritoneal membrane (Mem) were counted after abdominal surgery from each mouse treated with DMSO (n = 8) or TSAHC (n = 8) and graphed as the mean  $\pm$  standard deviation. Data represent three independent experiments. (F) Schematic model for TM4SF5-induced self-renewal capacity leading to CTC and liver-to-intestine metastases.

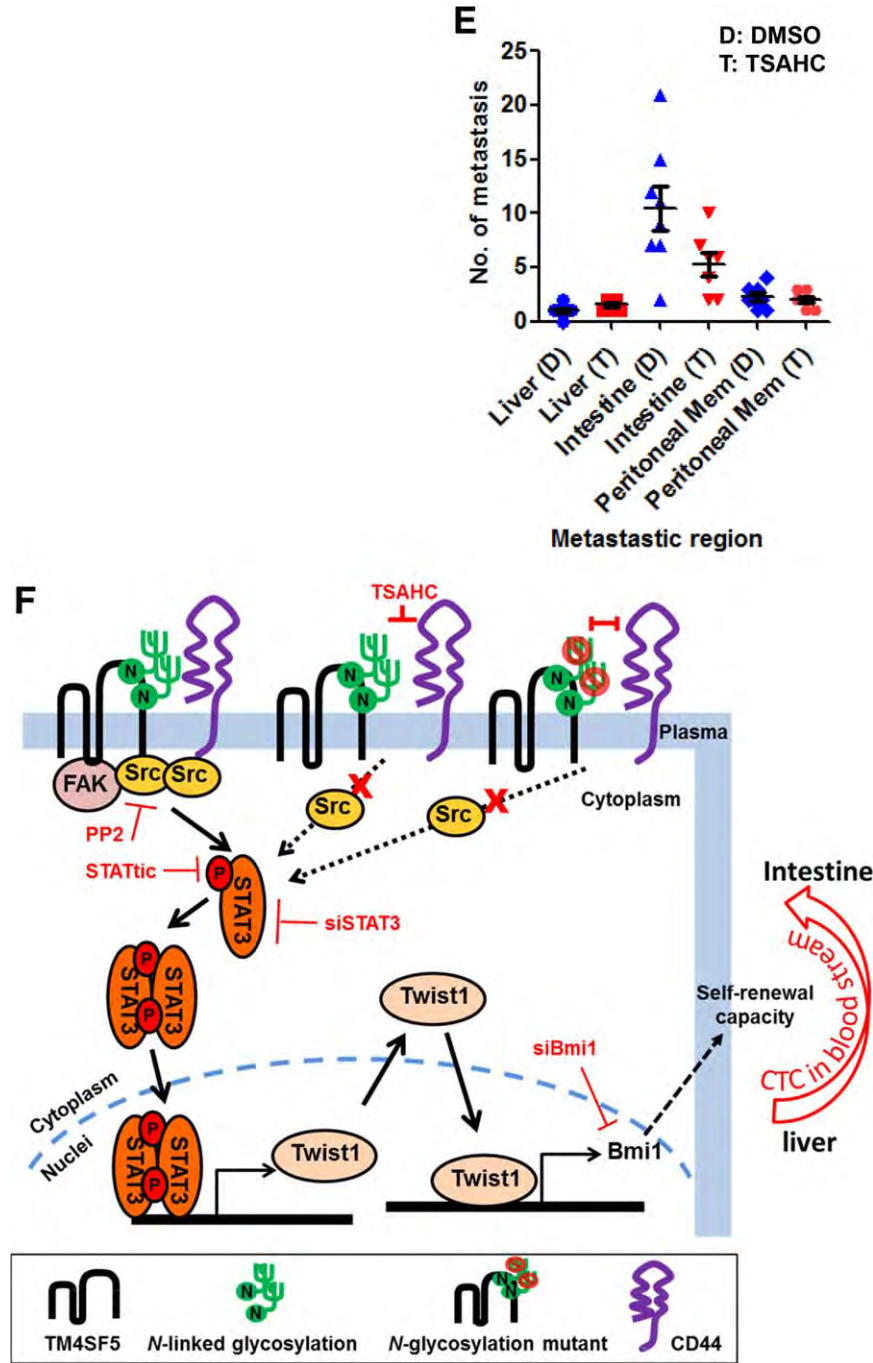


Fig. 8. (Continued)

cell-injected livers (8 of 8 mice; 100%) after a 2-week treatment, TSAHC treatment obviously inhibited metastatic cell populations (3 of 8 mice; 37.5%; Fig. 8A). Total signal flux from injected and metastatic cell populations were significantly reduced after 3 weeks of TSAHC treatment (Fig. 8B). We further evaluated metastasis after abdominal surgery (Fig. 8C). Quantitation after abdominal surgery showed a lower level of total flux in TSAHC-treated animals ( $P = 0.18$ ;  $n = 8$ ) and a significantly lower ( $P = 0.0287$ ;  $n = 8$ ) number

of the metastatic cell populations in TSAHC-treated animals, compared to DMSO-treated control mice (Fig. 8D). Metastatic populations were related mostly with the intestinal area and blocked by TSAHC treatments (Fig. 8E).

### Discussion

This study revealed that TM4SF5 bound CD44, and the interaction regulated levels or activities of c-

Src/STAT3/Twist1/Bmi1 to control the self-renewal properties of HCCs, subsequently promoting CTC capacity for metastasis (Fig. 8F). Furthermore, TM4SF5-dependent self-renewal and CTC properties were characterized by the molecular status of TM4SF5<sup>+</sup>/CD24<sup>-</sup>/CD44<sup>(TM4SF5-bound)</sup>/ALDH, leading to the c-Src/STAT3/Twist1/Bmi1 pathway. Knockdown or inhibition of any of these molecules inhibited self-renewal capacity. Whereas TM4SF5-expressing cells orthotopically injected into mouse livers were observed in blood and intestine of mice, knockdown of TM4SF5 or CD44, or inhibition of their interaction, abolished the detection of CTCs in the bloodstream and their colonization to distal organs such as intestine.

TM4SF5 is expressed in fibrotic livers after CCl<sub>4</sub> administration and its antagonist blocks chemically mediated liver fibrosis.<sup>17</sup> Mice administered chronic ethyl alcohol feeding for 4 weeks increased TM4SF5 expression in livers, and TM4SF5 transgenic mice showed fatty livers 12 months after birth (unpublished data). Transforming growth factor beta 1 (TGF- $\beta$ 1) or the conditioned media containing EGF from activated hepatic stellate cells causes small mothers against decapentaplegic (Smad)4 activation that leads to EGF receptor/extracellular-signal-regulated kinase (ERKs) signaling for TM4SF5 expression.<sup>18</sup> TGF $\beta$ 1, phospho-Smads, alpha-smooth muscle actin, collagen I, and TM4SF5 are costained along the fibrotic septa that run between the areas of the centrilobular bridging fibrosis in fibrotic livers, but not in control livers.<sup>17</sup> Furthermore, TM4SF5 is highly expressed in liver cancer tissues, compared to normal liver tissues.<sup>11</sup> Therefore, TM4SF5 appears to be expressed in pathological livers after chronic injuries, leading to gradual development of malignant fibrosis and tumorigenesis.

TM4SF5-dependent self-renewal properties could be related to TM4SF5-mediated EMT<sup>11</sup> and drug resistance.<sup>12</sup> The self-renewal property of metastatic cancer cells is important for tumor expansion after colonization at distal sites. Assuming that CTCs may be clinically important targets for drug development, the ability of TM4SF5 to mediate EMT, self-renewal, and CTC properties makes it a promising drug target. TM4SF5 may localize to tetraspan(in)-enriched microdomains (TEMs), where it can form massive protein complexes with integrins and growth factor receptors.<sup>10</sup> Protein complexes at TEMs may transduce signals that regulate diverse cellular functions.<sup>19</sup> In this current study, we showed that TM4SF5 interacted with CD44 through its extracellular domain, depending on the *N*-glycosylation status of TM4SF5. CD44

has been identified as a lymphocyte homing receptor<sup>20</sup> and also a proteoglycan that is also commonly expressed in epithelial and cancer cells.<sup>21</sup> CD44 is overexpressed in HCC for a poor prognosis,<sup>22,23</sup> and IHC of a limited number of clinical samples in our current study showed a regionally increased CD44 expression in liver cancer tissues, compared to matched-pair normal liver tissues. Diverse HCC cell lines differentially expressed CD44.<sup>24</sup> Although CD44 expression is also required for maintenance of stem cell phenotypes in breast cancer cells,<sup>25</sup> it has been suggested that CD44 can be more useful when combined with other markers to support for stemness in HCC.<sup>26</sup> Furthermore, the isoform conversion between standard CD44 (CD44s) and variant CD44 (CD44v) may be important for tumor initiation and maintenance.<sup>27</sup> Indeed, in our current study, we found that hepatic epithelial cells showed a comparable CD44 expression independent of TM4SF5 expression, and the open database of Oncomine also showed no significant difference in CD44 expression between normal and cancer liver samples, whereas TM4SF5 and Bmi1 were highly enhanced in cancer liver samples (Supporting Fig. 6). Although the relationship between TM4SF5 and CD44 protein levels in more clinical HCC tissues should be confirmed in future studies, it is likely that interaction between CD44 and TM4SF5 resulted in tumor-initiating and -circulating properties through the interaction-mediated signaling and the EMT phenotype.

TM4SF5 was previously shown to promote FAK<sup>28</sup> and c-Src activation,<sup>13</sup> and expression of the TM4SF5 *N*-glycosylation mutant or treatment with TSAHC abolished TM4SF5-mediated FAK/c-Src signaling and EMT.<sup>11</sup> Moreover, knockdown of either TM4SF5 or CD44 in SNU449T<sub>7</sub> cells decreased both c-Src and STAT3 phosphorylations, thereby inhibiting sphere growth. In the present study, c-Src acted upstream of STAT3 phosphorylation, as shown in a previous study.<sup>29</sup> STAT3 is activated in 50% of HCCs,<sup>30</sup> where STAT3 Tyr705 is phosphorylated in an interleukin-6-independent manner.<sup>31</sup> STAT3 signaling in HCCs can not only regulate genes involved in cell growth, survival, immune suppression, and angiogenesis, but also promote metastasis.<sup>32</sup> Highly activated STAT3 in HCCs binds to the promoter of the *Twist1* gene to increase *Twist1* mRNA expression.<sup>33</sup> Bmi1 is directly up-regulated by Twist1 and essential for Twist1-induced EMT,<sup>34</sup> and Bmi1 is also associated with stemness, leading to cancer recurrence and chemoresistance.<sup>35</sup> Moreover, Bmi1, which is up-regulated in many cancer types, is highly expressed in CD133<sup>+</sup>

murine liver CSCs<sup>36</sup> and enriched in CSCs with other stemness markers, including CD44,<sup>37</sup> being consistent with this current study. TM4SF5-mediated spheroid formation may not need CD90 or CD133, given that their expressions were not dependent on TM4SF5, although CD133 appears to act upstream of TM4SF5 (unpublished observations). Being consistent, CD133 and CD44 are considered markers for cancer stem cells in HCC.<sup>38,39</sup>

TSAHC has been shown not to cause any cytostatic effects in normal TM4SF5-negative hepatocytes.<sup>15,40</sup> Intraperitoneal TSAHC treatment given alone to mice (50 mg/kg<sup>-1</sup>) in 40% DMSO or orally (250 mg/kg<sup>-1</sup>) in 5% carboxymethyl cellulose for 4 weeks shows the anatomical appearance of livers comparable to control livers and does not cause any mortality, although TSAHC treatment together with CCl<sub>4</sub> administration decreases CCl<sub>4</sub>-mediated fibrotic phenotypes.<sup>17</sup> In the present study, TM4SF5-positive cells orthotopically injected into mice livers efficiently metastasized to intestine and peritoneal membrane, in addition to tail-vein-injected cells,<sup>41</sup> which were inhibited by the anti-TM4SF5 reagent, TSAHC. TM4SF5-mediated metastasis might have occurred through TM4SF5-dependent CTC properties supported by the TM4SF5/CD44/c-Src/STAT3/Twist1/Bmi1 pathway. Thus, it is likely that TM4SF5-positive cancer cells can circulate throughout blood and lymph nodes for eventual metastasis, and targeting TM4SF5 or interaction between TM4SF5 and CD44 may lead to efficient inhibition of TM4SF5-mediated metastasis.

## References

- Parkin DM, Bray F, Ferlay J, Pisani P. Global cancer statistics, 2002. *CA Cancer J Clin* 2005;55:74-108.
- Kassahun WT, Fangmann J, Harms J, Hauss J, Bartels M. Liver resection and transplantation in the management of hepatocellular carcinoma: a review. *Exp Clin Transplant* 2006;4:549-558.
- Kuvshinov BW, Ota DM. Radiofrequency ablation of liver tumors: influence of technique and tumor size. *Surgery* 2002;132:605-611.
- Lee JM, Dedhar S, Kalluri R, Thompson EW. The epithelial-mesenchymal transition: new insights in signaling, development, and disease. *J Cell Biol* 2006;172:973-981.
- Mani SA, Guo W, Liao MJ, Eaton EN, Ayyanan A, Zhou AY, et al. The epithelial-mesenchymal transition generates cells with properties of stem cells. *Cell* 2008;133:704-715.
- Thiery JP, Lim CT. Tumor dissemination: an EMT affair. *Cancer Cell* 2013;23:272-273.
- Brabletz T, Jung A, Spaderna S, Hlubek F, Kirchner T. Opinion: migrating cancer stem cells—an integrated concept of malignant tumour progression. *Nat Rev Cancer* 2005;5:744-749.
- Dean M, Fojo T, Bates S. Tumour stem cells and drug resistance. *Nat Rev Cancer* 2005;5:275-284.
- Tiwari N, Gheldof A, Tatari M, Christofori G. EMT as the ultimate survival mechanism of cancer cells. *Semin Cancer Biol* 2012;22:194-207.
- Lee SA, Park KH, Lee JW. Modulation of signaling between TM4SF5 and integrins in tumor microenvironment. *Front Biosci* 2011;16:1752-1758.
- Lee SA, Lee SY, Cho IH, Oh MA, Kang ES, Kim YB, et al. Tetraspanin TM4SF5 mediates loss of contact inhibition through epithelial-mesenchymal transition in human hepatocarcinoma. *J Clin Invest* 2008;118:1354-1366.
- Lee MS, Kim HP, Kim TY, Lee JW. Gefitinib resistance of cancer cells correlated with TM4SF5-mediated epithelial-mesenchymal transition. *Biochim Biophys Acta* 2012;1823:514-523.
- Jung O, Choi YJ, Kwak TK, Kang M, Lee MS, Ryu J, et al. The COOH-terminus of TM4SF5 in hepatoma cell lines regulates c-Src to form invasive protrusions via EGFR Tyr845 phosphorylation. *Biochim Biophys Acta* 2013;1833:629-642.
- Choi S, Oh SR, Lee SA, Lee SY, Ahn K, Lee HK, Lee JW. Regulation of TM4SF5-mediated tumorigenesis through induction of cell detachment and death by tiaralic acid. *Biochim Biophys Acta* 2008;1783:1632-1641.
- Lee SA, Ryu HW, Kim YM, Choi S, Lee MJ, Kwak TK, et al. Blockade of four-transmembrane L6 family member 5 (TM4SF5)-mediated tumorigenicity in hepatocytes by a synthetic chalcone derivative. *HEPATOLOGY* 2009;49:1316-1325.
- Kim HP, Kim TY, Lee MS, Jong HS, Kim TY, Weon Lee J, Bang YJ. TGF- $\beta$ 1-mediated activations of c-Src and Rac1 modulate levels of cyclins and p27Kip1 CDK inhibitor in hepatoma cells replated on fibronectin. *Biochim Biophys Acta* 2005;1743:151-161.
- Kang M, Jeong SJ, Park SY, Lee HJ, Kim HJ, Park KH, et al. Antagonistic regulation of transmembrane 4 L6 family member 5 attenuates fibrotic phenotypes in CCl<sub>4</sub>-treated mice. *FEBS J* 2012;279:625-635.
- Kang M, Choi S, Jeong SJ, Lee SA, Kwak TK, Kim H, et al. Cross-talk between TGF $\beta$ 1 and EGFR signalling pathways induces TM4SF5 expression and epithelial-mesenchymal transition. *Biochem J* 2012;443:691-700.
- Hemler ME. Tetraspanin proteins mediate cellular penetration, invasion, and fusion events and define a novel type of membrane microdomain. *Annu Rev Cell Dev Biol* 2003;19:397-422.
- Gallatin WM, Weissman IL, Butcher EC. A cell-surface molecule involved in organ-specific homing of lymphocytes. *Nature* 1983;304:30-34.
- Williams K, Motiani K, Giridhar PV, Kasper S. CD44 integrates signaling in normal stem cell, cancer stem cell and (pre)metastatic niches. *Exp Biol Med (Maywood)* 2013;238:324-338.
- Endo K, Terada T. Protein expression of CD44 (standard and variant isoforms) in hepatocellular carcinoma: relationships with tumor grade, clinicopathologic parameters, p53 expression, and patient survival. *J Hepatol* 2000;32:78-84.
- Mima K, Okabe H, Ishimoto T, Hayashi H, Nakagawa S, Kuroki H, et al. CD44s regulates the TGF- $\beta$ -mediated mesenchymal phenotype and is associated with poor prognosis in patients with hepatocellular carcinoma. *Cancer Res* 2012;72:3414-3423.
- Okabe H, Ishimoto T, Mima K, Nakagawa S, Hayashi H, Kuroki H, et al. CD44s signals the acquisition of the mesenchymal phenotype required for anchorage-independent cell survival in hepatocellular carcinoma. *Br J Cancer* 2014;110:958-966.
- Pham PV, Phan NL, Nguyen NT, Truong NH, Duong TT, Le DV, et al. Differentiation of breast cancer stem cells by knockdown of CD44: promising differentiation therapy. *J Transl Med* 2011;9:209.
- Liu LL, Fu D, Ma Y, Shen XZ. The power and the promise of liver cancer stem cell markers. *Stem Cells Dev* 2011;20:2023-2030.
- Prochazka L, Tesarik R, Turanek J. Regulation of alternative splicing of CD44 in cancer. *Cell Signal* 2014;26:2234-2239.
- Jung O, Choi S, Jang SB, Lee SA, Lim ST, Choi YJ, et al. Tetraspanin TM4SF5-dependent direct activation of FAK and metastatic potential of hepatocarcinoma cells. *J Cell Sci* 2012;125:5960-5973.
- Schaefer LK, Wang S, Schaefer TS. c-Src activates the DNA binding and transcriptional activity of Stat3 molecules: serine 727 is not

- required for transcriptional activation under certain circumstances. *Biochem Biophys Res Commun* 1999;266:481-487.
30. Subramaniam A, Shanmugam MK, Perumal E, Li F, Nachiyappan A, Dai X, et al. Potential role of signal transducer and activator of transcription (STAT)3 signaling pathway in inflammation, survival, proliferation and invasion of hepatocellular carcinoma. *Biochim Biophys Acta* 2013;1835:46-60.
  31. Ryu J, Kang M, Lee MS, Kim HJ, Nam SH, Song HE, et al. Crosstalk between the TM4SF5/FAK and the IL6/STAT3 pathways renders immune escape of human liver cancer cells. *Mol Cell Biol* 2014;34:2946-2960.
  32. Li WC, Ye SL, Sun RX, Liu YK, Tang ZY, Kim Y, et al. Inhibition of growth and metastasis of human hepatocellular carcinoma by antisense oligonucleotide targeting signal transducer and activator of transcription 3. *Clin Cancer Res* 2006;12:7140-7148.
  33. Cheng GZ, Zhang WZ, Sun M, Wang Q, Coppola D, Mansour M, et al. Twist is transcriptionally induced by activation of STAT3 and mediates STAT3 oncogenic function. *J Biol Chem* 2008;283:14665-14673.
  34. Yang MH, Hsu DS, Wang HW, Wang HJ, Lan HY, Yang WH, et al. Bmi1 is essential in Twist1-induced epithelial-mesenchymal transition. *Nat Cell Biol* 2010;12:982-992.
  35. Cao L, Bombard J, Cintron K, Sheedy J, Weetall ML, Davis TW. BMI1 as a novel target for drug discovery in cancer. *J Cell Biochem* 2011;112:2729-2741.
  36. Oishi N, Wang XW. Novel therapeutic strategies for targeting liver cancer stem cells. *Int J Biol Sci* 2011;7:517-535.
  37. Siddique HR, Saleem M. Role of BMI1, a stem cell factor, in cancer recurrence and chemoresistance: preclinical and clinical evidences. *Stem Cells* 2012;30:372-378.
  38. Zhu Z, Hao X, Yan M, Yao M, Ge C, Gu J, Li J. Cancer stem/progenitor cells are highly enriched in CD133+CD44+ population in hepatocellular carcinoma. *Int J Cancer* 2010;126:2067-2078.
  39. Pang RW, Poon RT. Cancer stem cell as a potential therapeutic target in hepatocellular carcinoma. *Curr Cancer Drug Targets* 2012;12:1081-1094.
  40. Lee SA, Lee MS, Ryu HW, Kwak TK, Kim H, Kang M, et al. Differential inhibition of transmembrane 4 L six family member 5 (TM4SF5)-mediated tumorigenesis by TSAHC and sorafenib. *Cancer Biol Ther* 2011;11:330-336.
  41. Lee SA, Kim TY, Kwak TK, Kim H, Kim S, Lee HJ, et al. Transmembrane 4 L six family member 5 (TM4SF5) enhances migration and invasion of hepatocytes for effective metastasis. *J Cell Biochem* 2010;111:59-66.
  42. Kang M, Ryu J, Lee D, Lee MS, Kim HJ, Nam SH, et al. Correlations between Transmembrane 4 L6 family member 5 (TM4SF5), CD151, and CD63 in liver fibrotic phenotypes and hepatic migration and invasive capacities. *PLoS ONE* 2014;9:e102817.

## Supporting Information

Additional Supporting Information may be found at [onlinelibrary.wiley.com/doi/10.1002/hep.27721/supinfo](http://onlinelibrary.wiley.com/doi/10.1002/hep.27721/supinfo).